Beam compression experiments using the UCLA/ATF compressor

J.B. ROSENZWEIG[¥], M. DUNNING[¥], E. HEMSING[¥], G. ANDONIAN[¥], A.M. COOK[¥], A. MUROKH[¥], S. REICHE[¥], D. SCHILLER[¥], M. BABZIEN[#], K. KUSCHE[#], V. YAKIMENKO[#], L. PALUMBO[#], C. VICARIO[#]

[¥]UCLA Dept. of Physics and Astronomy, 405 Hilgard Ave., Los Angeles, CA 90034, USA
[#]Accelerator Test Facility, Brookhaven National Laboratory, Upton, NY 11973, USA
[£]Istituto Nazionale di Fisica Nucleare, Laboratori Nazionale di Frascati, Frascati (RM) Italy

Abstract. We review recent experimental results from the BNL ATF using the compressor built by UCLA. The measurements discussed include: first observation of short wavelength coherent edge radiation angular/wavelength spectrum and spectrum, sub-100 fsec pulse-length coherent transition autocorrelation measurements, and longitudinal and transverse phase space distortions. Extension of these measurements, as well as those which can be made possible by a new X-band traveling wave deflector being developed in an industrial collaboration, are examined.

Keywords: chicane compression, synchrotron radiation, coherent radiation, edge radiation.
PACS: 52.59.Rz, 41.75.Fr, 52.59.Sa, 41.60.Bq

INTRODUCTION

The UCLA-designed and built chicane compressor at the BNL ATF [1], installed in the high-energy beam line after the injector, has been used for a number of fundamental beam physics in the past year, as well as in applications [2] such a plasma wakefield acceleration [3]. The compression experiments a have emphasized both creation of very short (as short as 25 microns rms) beam pulses, and on measuring the characteristics of coherent synchrotron radiation (CSR) and of coherent edge radiation (CER) emitted from such short beams.

While much of the recent work on radiation from chicanes has centered on CSR due to the possibility of CSR-induced microbunching instability in linear colliders and short wavelengths FELS, the closely related CER effect has not yet been observed in the relevant short wavelength regime. In addition, because of the flat CER power dependence on frequency [4], it may be used in a non-destructive beam monitoring scheme, as has been proposed for the LCLS [5]. CER has also been shown to be a bright source of infrared radiation, which makes it well-suited for types of microscopy and spectroscopy [6].

To examine the physics of CER from compressed beams, we have put together a measurement program based on cryogenic detectors for the copious THz radiation expected from the compressor. In order to model the experiment, a start-to-end simulation, formed from UCLA PARMELA [7], Elegant [8] and a new Lenard-Wiechert far-field calculation code termed QUINDI, has been put together which allows the general behavior of the system to be predicted.

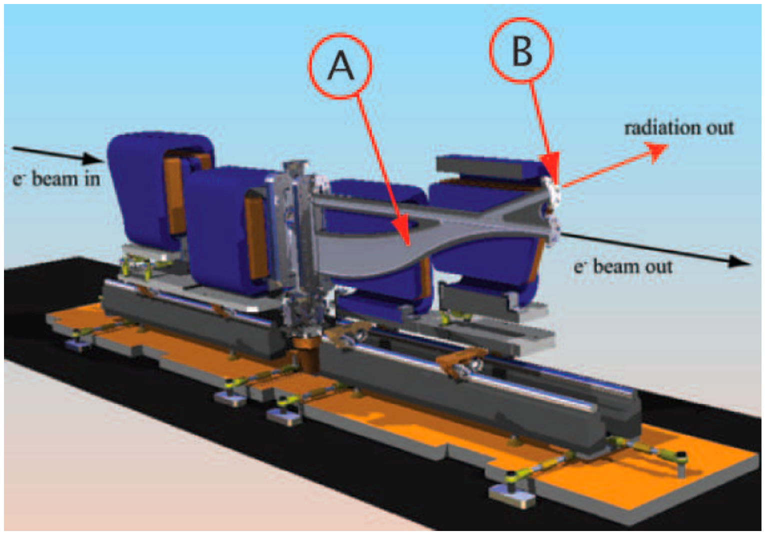

Figure 1. Rendering of the UCLA-built ATF chicane compressor Cutaway view shows the radiation source region between the third and fourth dipoles (A) and the radiation extraction port (B).

The compression process creates sub-30 micron long beams by use of the magnetic chicane, shown in Fig. 1. In addition to the double-focusing chicane magnets, a custom vacuum-vessel was constructed which allows beam diagnosis in chicane-on and –off configurations, and also features a dedicated coherent radiation port that points backward to the constructively interfering CER creation regions at the exit of the third magnet/entrance to the final magnet. At this point, the beam is roughly as short as it is at the exit of the chicane, and the switching of bend from one direction to the other at these edges gives a large advantage to the measurement of CER, which is absent in any storage ring, where the edges are destructively interfering [9].

The modeling of the beam dynamics in the chicane system was undertaken first by ELEGANT, with the usual UCLA PARMELA-modeled beam particles at accelerator exit used as input. This combination has proven extremely successful in UCLA led experiments on FEL at the ATF previously [10]. In order to deduce the spectrum of coherent radiation expected from the compressor, an additional based code was written and deployed in the past year, QUINDI. Both analytical models as well as QUINDI, give insight into the unique aspects of CER radiation at short wavelengths. When a charged particle encounters a fast changing magnetic field (edge), it emits an enhanced radiation-spectrum that is similar to transition radiation (TR), with *radial* polarization as opposed to nearly linear polarization found in CSR. It also has a TR-like off-axis radiation angular distribution. In order for CER to be significant the field change must occur on a scale much shorter than a radiation formation length. In addition, it is expected that the CER wavelength dependence in this spectral region will differ from that of CSR in a systematic way, having enhanced long wavelength components. Thus for long wavelengths (0.1-2 mm) the radiation appears at the detection window in our experiment as a TR-like pattern while at shorter wavelengths (optical to near IR), the spectrum is not distinguishable from synchrotron radiation.

EXPERIMENTAL RESULTS

The first measurements at the chicane were made on phase space effects. In particular, transverse phase space tomography measurements showed phase space bifurcation at 60 MeV [11]. This indicated that the velocity fields, which were dominant in previous Neptune experiments at 12 MeV [12], still impact the ATF measurements. Along with the slight bifurcation of transverse phase space, there was a much more dramatic breakup in the momentum spectrum, which is directly affected by collective fields. The strong splitting of the momentum distribution, which has been observed in previous experiments at, e.g., TTF, is seen in the spectrometer at the phase of full compression, as shown in Fig. 2.

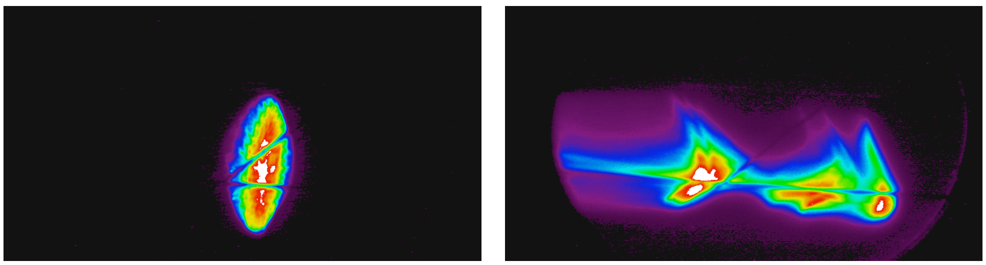

Figure 2. Beam images in the spectrometer, (bend plane is horizontal): (left) 9° forward of RF crest near minimum energy spread, no compression, (right) 19° forward of crest, maximum compression.

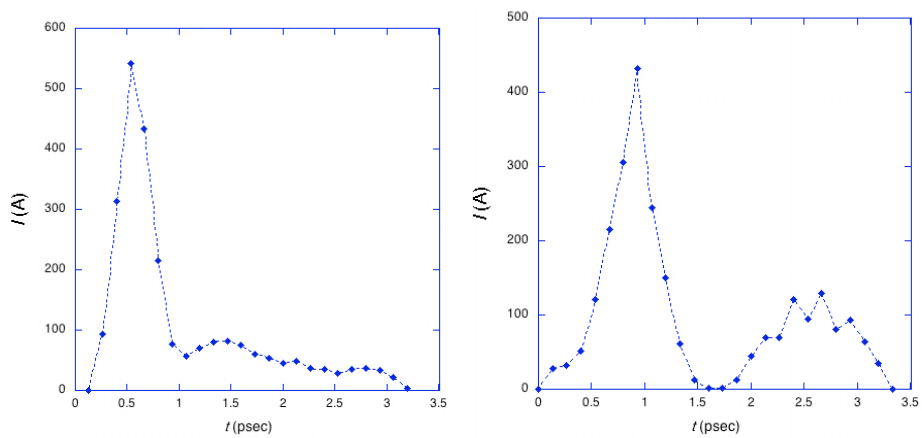

Figure 3. Reconstructed longitudinal beam profiles using Kramers-Kronig analysis of CTR: (left) optimum compression, (right) over compression.

To further explore the longitudinal dynamics in the chicane, CTR interferometry was performed. In the past year, we have gained expertise in the use of Kramers-Kronig analysis to reconstruct the time-domain profile of the bunch, which requires assumption of minimal phase, as proposed by Lai and Sievers [13]. Examples of such reconstructions are shown in Fig. 3, in which the characteristic one-sided distribution, with small evidence for splitting of the beam, shows up at optimal compression. Note that the directionality of the asymmetry is not determined in the Kramers-Kronig reconstruction. With over-compression the beam displays distinct splitting in the time profile. This is because the beam is fully compressed within the third dipole, suffers strong energy and trajectory-changing forces there, and then significantly rearranges in the remaining bending path. This splitting has been observed in wakefield experiments performed recently at the ATF [2].

Much recent activity at the compressor has been dedicated to observation of CER. The existence of out-of-bend-plane radiation — π-polarization — in addition to in plane, or σ-polarization, has been verified in detail, as shown in Fig. 4. This type of polarization pattern is correlated with the far-field angular distribution, which was measured by use of point-to-parallel optics, followed by movable iris collimation, before the collection of the CER at the cryogenic bolometer. Scans of such distributions were made as a function of polarizer angle, and these are shown in Fig. 4. The addition of π-polarization is displayed as an offset in the intensity dependence on angle. Purely radial (equal π and σ) polarization is not observed for two reasons: the magnetic edge transition is not "zero-length" [9], and the collection acceptance allows some amount of radiation from regions nearby to the edge transition. To quantify both of these effects, we must rely on simulation. The predicted polarization of the collected from QUINDI is shown as well in Fig. 4; the agreement is quite good.

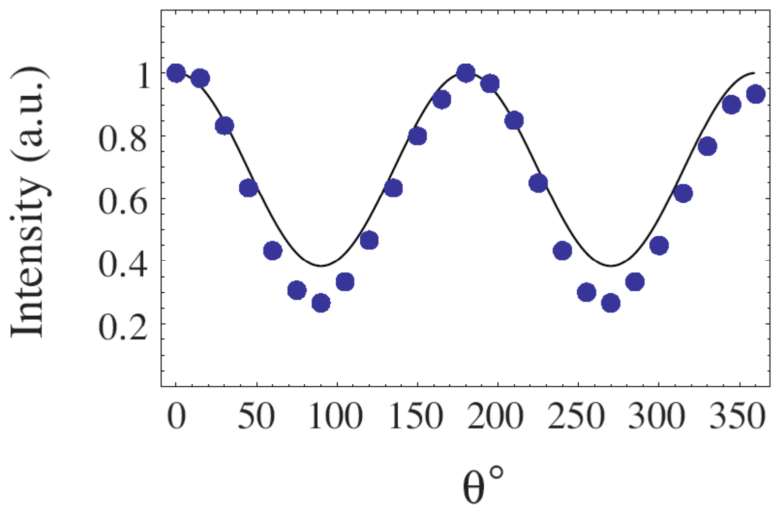

Figure 4. Polarization scan of CER at UCLA/ATF compressor, taken under maximum compression conditions. Solid line is the prediction of QUINDI.

In addition to these distributions, CER should be characterized in terms of wavelength spectral intensity. Attempts were made to accomplish this by use of low-pass filters, but these proved difficult to calibrate and interpret. Also a custom diffraction-grating based spectrometer was built, but the gratings themselves did not have adequate THz behavior. In the end, we have employed the same Michelson autocorrelation scheme as used for the CTR in characterizing the CER, but using the cold bolometer as the detector instead of Golay cells. Because of dispersion (and associated absorption lines) in the air transport, the autocorrelation displays a wave train, as seen in Fig. 5.

The wavelength spectrum deduced from this measurement via FFT (including a windowing function, *cf.* Fig. 5), is shown in Fig. 6, along with the predictions of QUINDI. For reference, we also show the position of water absorption lines in Fig. 6; they coincide well with local minima in the observed spectra.

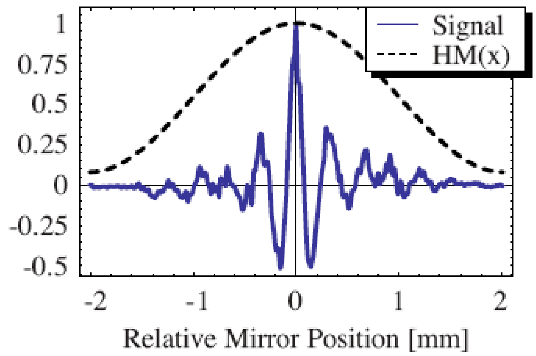

Figure 5. (left) Autocorrelation of CER using Michelson interferometer and cryogenic bolometer, along with Hamming window function for apodizing FFT.

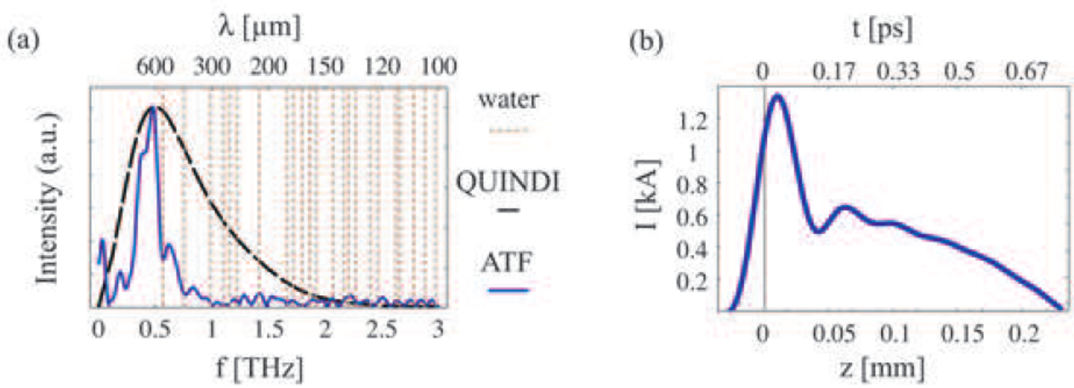

Figure 6. (a) Spectra from apodized interferogram and from QUINDI simulation. Prominent water absorption frequencies are shown as vertical dotted lines. (b) Minimal phase Kramers-Kronig bunch reconstruction for the measured spectrum.

Despite the dispersion of the collection system, the Kramers-Kronig analysis, which depends only on the amplitude information and not the phase of the autocorrelation, still should be valid, to the extent that not too much frequency information is missing due to absorption. Such a reconstruction is shown in Fig. 6; the bunch time profile is in decent agreement with the CTR measurement of Fig. 3.

The far-field distribution intensity distribution of CER is also quite different than that of synchrotron radiation. The CTR-like angular dependence of the CER is highly correlated to its polarization, as so we have measured, using point-to-parallel collection optics after the source [1], and a movable collimating iris just before the final collecting lens. The angular distributions thus obtained are shown in Fig. 7.

In order to compare the CER angular measurements with the start-to-end simulations culminating in QUINDI, some intermediate steps are required, as much of the frequency spectrum above 1 THz is distorted during propagation in the atmosphere, as well as in the output port fused silica window. The spectral information obtained from the autocorrelator measurements was used to deduce an efficiency of radiation collection, which was then used to normalize the far-field angular flux distribution predicted by QUINDI.

The predictions derived from QUINDI in this manner are shown in Fig. 7, with the simulated iso-intensity contours overlaid upon the observed intensity distribution shown in a false color map. The agreement in many of the features between simulation and measurement is striking, especially given that the observed radiation has quite long wavelength, and therefore the nearby metallic boundary of the vacuum vessel may have a significant effect on the creation and subsequent propagation of the CER.

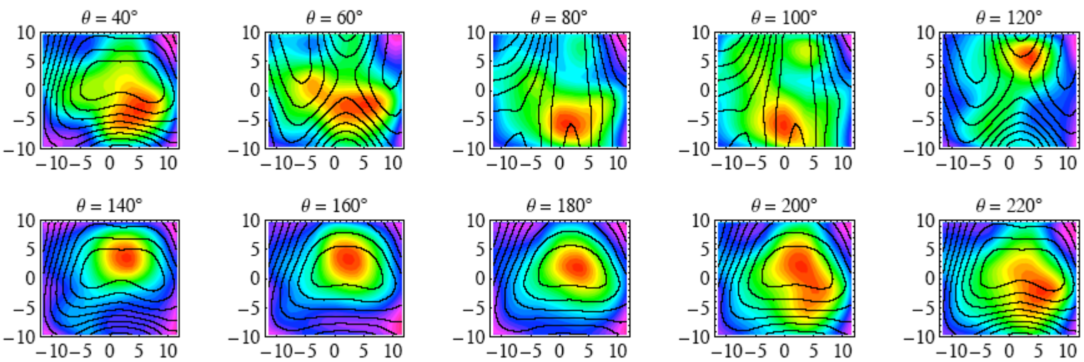

Figure 7. CER far-field angular distributions as a function of polarizer angle in UCLA/ATF compressor, taken under maximum compression conditions.

FUTURE PLANS

In the near future, more detailed measurements, with care taken to eliminate absorption in transport, of the radiation from the compressed beam is planned. Further downstream, we plan to take an active role in the X-band RF deflector measurements at the ATF, in collaboration with an industrial partner, RadiaBeam Technologies. One area of collaboration that UCLA took part in during the X-band deflector phase I SBIR work was in experiment simulations. In particular, start-to-end simulations dedicated to modeling the implementation of the RF deflector in the phase II experiments at the ATF have been performed using UCLA PARMELA and Elegant. The simulation of the deflector performance in its simplest configuration just downstream of the RF deflector gives *2 fsec* resolution.

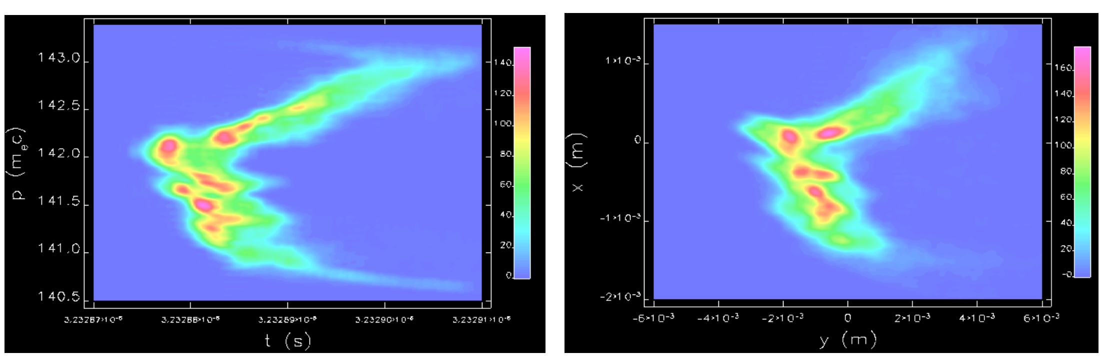

Figure 8. (top) The simulated longitudinal phase space after the chicane compressor at the ATF (Q=0.3 nC); (bottom) a simulated beam image (x,y) in the longitudinal phase space measurement system based on RF deflector and bend magnet.

We have also examined the more challenging and interesting implementation of longitudinal phase space measurement at the ATF. In this case, the beam traverses the vertically bending chicane, the vertically sweeping X-band deflector, and the 20° horizontally bending dipole at the end of the high energy injector line, followed by a drift of 80 cm to a beam-imaging detector. The transverse (x,y) beam image at the detector in the longitudinal phase space measurement is shown in Fig. 8 with the pre-bend (at the deflector) longitudinal phase space shown for comparison. The general features of the longitudinal phase space are reproduced, including filamentation amplified by the effects of CSR.

The agreement between the two distributions shown in Fig. 8 is quite good, having only a bit of systematic distortion in the *p-t* mapping, at the 10 fsec level. This distortion arises from the effects of CSR, which changes the electron energy in a notable way for such a short beam undergoing bending. Fortunately, the energy change, even though it accumulates significantly by the end of the CSR interaction (which extends past the dipole exit), does not strongly effect the momentum dispersion, and thus the (x,y) distribution in Fig. 8. The distortion of the momentum spectrum by CSR in the bend implies that this diagnostic is operated near the limit of its physical applicability. We plan to investigate this further, using codes that include not only CSR (Elegant has only a rudimentary 1D model), but also velocity fields. The simulation code currently used, TREDI, employs a three-dimensional point-by-point Lenard-Wiechert field-based model, which means that it is extremely computationally intensive to model self-consistent dynamics in this way. We are therefore evaluating alternative approaches to these simulations.

ACKNOWLEDGMENTS

This work is partially supported by the US Dept. of Energy under grant DE-FG03-92ER40693, the National Science Foundation, and by the EU Commission in the 6th framework program, contract no. 011935 EUROFEL-DS1.

REFERENCES

1. G. Andonian, *et al.,* Proceedings of the 2003 Particle Accelerator Conference, 944 (2003).
2. V. Yakimenko, private communication.
3. J.B. Rosenzweig, N. Barov and E. Colby, *IEEE Trans. Plasma Sci.* **24,** 409 (1996)
4. O. V. Chubar and N. V. Smolyakov, *J. Optics (Paris)* 24, 117 (1993).
5 . M. Dunning, et al., in *Physics and Applications of High Brightness Electron Beams, Eds. L. Palumbo, J.B. Rosenzweig, L. Serafini* (World Scientific, 2006).
6. T. E. May, R. A. Bosch and R. L. Julian, Proc. 1999 Part. Accelerator Conf., 2394 (1999).
7. E. Colby, *UCLA PhD Thesis*, FERMILAB-THESIS-1997-03 (FNAL, 1997).
8. M. Borland, *Proceedings of the 2000 International LinacConference*, 833 (2001).
9. R. A. Bosch, *Il Nuovo Cimento* 20D, 483 (1998).
10. A. Murokh*, et al., Physical Review E* **67**, 066501 (2003); G. Andonian, *et al., Phys. Rev Lett.* **95,** 054801 (2005)
11. F. Zhou, et al., submitted to *Physical Review Letters*.
12. S.G. Anderson, *et al., Phys. Rev. Lett***. 91** , 074803 (2003)
13. R. Lai and A.J. Sievers, *Phys. Rev. E* 50, 5 (1994).